SCIENCE CHINA
Chemistry

• ARTICLES •
· SPECIAL ISSUE · Green Chemistry

doi: 10.1007/s11426-016-0489-3

Efficient aerobic oxidation of 5-hydroxymethylfurfural to 2,5-furandicarboxylic acid on Ru/C catalysts

Lufan Zheng[1], Junqi Zhao[1], Zexue Du[1], Baoning Zong[1*] & Haichao Liu[2*]

[1]*Research Institute of Petroleum Processing, SINOPEC, Beijing 100083, China*
[2]*Beijing National Laboratory for Molecular Sciences, State Key Laboratory for Structural Chemistry of Stable and Unstable Species, College of Chemistry and Molecular Engineering, Peking University, Beijing 100871, China*

Received November 23, 2016; accepted January 5, 2017; published online May 9, 2017

2,5-Furandicarboxylic (FDCA) is a potential substitute for petroleum-derived terephthalic acid, and aerobic oxidation of 5-hydroxymethylfurfural (HMF) provides an efficient route to synthesis of FDCA. On an activated carbon supported ruthenium (Ru/C) catalyst (with 5 wt% Ru loading), HMF was readily oxidized to FDCA in a high yield of 97.3% at 383 K and 1.0 MPa O_2 in the presence of $Mg(OH)_2$ as base additive. Ru/C was superior to Pt/C and Pd/C and also other supported Ru catalysts with similar sizes of metal nanoparticles (1–2 nm). The Ru/C catalysts were stable and recyclable, and their efficiency in the formation of FDCA increased with Ru loadings examined in the range of 0.5 wt%–5.0 wt%. Based on the kinetic studies including the effects of reaction time, reaction temperature, O_2 pressure, on the oxidation of HMF to FDCA on Ru/C, it was confirmed that the oxidation of HMF to FDCA proceeds involving the primary oxidation of HMF to 2,5-diformylfuran (DFF) intermediate, and its sequential oxidation to 5-formyl-2-furancarboxylic acid (FFCA) and ultimately to FDCA, in which the oxidation of FFCA to FDCA is the rate-determining step and dictates the overall formation rate of FDCA. This study provides directions towards efficient synthesis of FDCA from HMF, for example, by designing novel catalysts more efficient for the involved oxidation step of FFCA to FDCA.

aerobic oxidation, 5-hydromethylfurfural, 2,5-furandicarboxylic, supported Ru catalyst, base additives, reaction mechanism

Citation: Zheng L, Zhao J, Du Z, Zong B, Liu H. Efficient aerobic oxidation of 5-hydroxymethylfurfural to 2,5-furandicarboxylic acid on Ru/C catalysts. *Sci China Chem*, 2017, 60, doi: 10.1007/s11426-016-0489-3

1 Introduction

Biomass is renewable and largely available in nature, and it provides the most viable alternative to fossil fuels for sustainable production of liquid fuels and organic chemicals [1,2]. 5-Hydroxymethylfurfural (HMF), as one of the important biomass-based platform molecules, has attracted increasing attention over the past decade. It can be synthesized by acid-catalyzed dehydration of carbohydrates, such as fructose, glucose and cellulose [3–5], and converted to a variety of bulk chemicals and intermediates, such as 2,5-furandicarboxylic acid (FDCA) and 2,5-diformylfuran (DFF) [6–8].

FDCA has a similar conjugated structure to terephthalic acid (PTA), and it is considered as a potential substitute for PTA towards the sustainable production of polyamides and polyesters [9]. In attempts to achieve efficient aerobic oxidation of 5-hydroxymethylfurfural (HMF) to FDCA, a large number of homogeneous (e.g. Co/Mn/Br) and heterogeneous catalysts (e.g. Pt, Au, Pd and Ru-based catalysts) have been explored [10–19]. Pt, Au and Pd-based catalysts usually re-

*Corresponding authors (email: zongbn.ripp@sinopec.com; hcliu@pku.edu.cn)

quire aqueous alkali solutions to obtain high yields of FDCA. For example, Ait Rass *et al*. [17] reported an almost quantitative yield of FDCA on Pt-Bi/C catalyst at 373 K and 4 MPa air in a Na_2CO_3 solution. On Au-Cu/TiO_2 catalyst, Pasini *et al*. [18] obtained FDCA yields of 90%–99% at 368 K and 1 MPa O_2 in the presence of NaOH. The presence of alkali or other base additives can prevent strong adsorption of FDCA onto the noble metal surfaces and their consequent deactivation, which can also neutralize and stabilize FDCA. Moreover, the basic conditions can facilitate the hydration of aldehyde intermediates to the corresponding germinal diol intermediates and their oxidation to FDCA [17].

Compared with Pt, Pd and Au, Ru is much cheaper. Ru-based catalysts exhibit excellent performance in the selective oxidation of alcohols, and have now been applied to the aerobic oxidation of HMF to FDCA. Gorbanev *et al*. [20] loaded $Ru(OH)_x$ on hydrotalcite (HT), showing 95% yield of FDCA after HMF oxidation at 413 K for 6 h in water without addition of alkali additive. However, the catalyst tended to deactivate due to the decomposition of HT support and Ru leaching. Artz and Palkovits [21] compared supported Ru catalysts on covalent triazine frameworks and commercial Ru/C catalysts, and found the superiority of Ru/CTF-c to Ru/C in term of the FDCA yield (77.6% vs. 62.8%) under the same reaction conditions. Interestingly, they also found that for the commercial Ru/C catalysts, without being washed with dimethyl sulfoxide (DMSO) before use, the FDCA yield decreased significantly (from 62.8% to 41.4%). Zhang and coworkers [22] reported base-free HMF oxidation to FDCA in 88% yield on commercial Ru/C catalysts (HMF/Ru (molar ratio)=10) after reaction at 393 K for 10 h, notwithstanding the observed activity loss imposed by strong adsorption of FDCA on the Ru surfaces.

Recently, we reported that Ru/C efficiently catalyzed the oxidation of HMF to DFF with a high yield of 96% in toluene [23], and to FDCA with a moderate yield of 78% in water upon addition of hydrotalcite (HT) base (Mg/Al=3) [24,25]. This work presents a systematic study on the synthesis of FDCA from the aerobic oxidation of HMF on Ru/C in the presence of base additives. We compared the performances of Ru/C and C-supported Ru, Pt and Pd catalysts and also different supported Ru catalysts. To better understand the functions of base additives, we investigated some representative solid oxides and hydroxides with basicity (MgO, $Mg(OH)_2$, La_2O_3, Al_2O_3, $Al(OH)_3$, and also HT with different Mg/Al ratios) as well as alkaline compounds (NaOH, $CaCO_3$, and Na_2CO_3). We also examined the effects of reaction parameters including reaction temperature, O_2 pressure and reaction time on the oxidation of HMF to FDCA. Finally, we discussed the reaction pathways for the oxidation of HMF to FDCA, and confirm DFF instead of 5-hydroxymethyl-2-furancarboxylic acid (HMFCA) as the key intermediate for the formation of FDCA.

2 Experimental

2.1 Catalyst preparation and characterization

Activated carbon supported Ru, Pt, Pd catalysts were prepared by an incipient wetness impregnation method. Briefly, activated carbon (Sinopharm Chemical, China) was dried at 393 K overnight in air, into which aqueous solutions of $RuCl_3{\cdot}nH_2O$ (Sinopharm Chemical, China), $H_2PtCl_6{\cdot}6H_2O$ (Sinopharm Chemical, China), $PdCl_2$ (Sinopharm Chemical, China; with 0.5 mL of concentrated aqueous HCl solution) were added in turn at 298 K. After impregnation for 6 h, the catalysts were dried overnight in air at 383 K, and then reduced in a flowing gas of 20% H_2/N_2 at 673 K for 4 h.

Following the similar impregnation procedures, metal oxide-supported Ru catalysts were also prepared. The supports included ZrO_2 (Sinopharm Chemical, China), Al_2O_3 (Sinopharm Chemical, China) and TiO_2 (J&K Scientific, China), and they were calcined at 673 K in air prior to use.

Base additives, including MgO, Al_2O_3, $Al(OH)_3$, $Mg(OH)_2$, $CaCO_3$, NaOH, Na_2CO_3 and La_2O_3 were purchased from Sinopharm Chemical, China. Hydrotalcite samples with different Mg/Al molar ratios were prepared by a homogenous co-precipitation method, as described in our previous work [25].

Transmission electron microscope (TEM) images were taken on a Philips Tecnai F30 FEG-TEM (Netherlands) at 300 kV. The catalysts were dispersed in ethanol uniformly and then placed on carbon-coated Cu grids. The average sizes and the size distribution of metal particles were obtained by counting at least 300 particles randomly from the TEM images.

2.2 Selective oxidation of HMF to FDCA

Oxidation reactions of HMF were carried out in a Teflon-lined stainless steel autoclave (100 mL), equipped with a mechanical stirrer and temperature measurement gauges. In a typical run, 1 mg HMF (98%, Alfa Aesar, USA), 0.04 g Ru/C and 0.2 g $Mg(OH)_2$ were introduced into an autoclave (100 mL) containing 20 mL deionized H_2O. The autoclave was then pressurized to 1.0 MPa with oxygen, and heated from 298 K to 383 K with vigorous stirring at a speed of 700 r/min during the reaction to eliminate the mass-transfer limitation. After the reaction, the catalysts were removed by filtration, and the reactants and products were analyzed by a high-performance liquid chromatography (HPLC; Shimadzu LC-20A, Japan) using an UV detector and an Alltech OA-1000 (USA) organic acid column (with a mobile phase of 0.005 M H_2SO_4, at a flow rate of 0.6 mL/min and an oven temperature of 343 K). In the recycling experiments, the used catalysts were washed thoroughly with deionized water and dried in air at 343 K before the next cycle. After each cycle, about 30% more $Mg(OH)_2$ was added to compensate the consumption from its reaction

with the carboxylic acid products. The HMF conversion and product selectivity are calculated as follows:

$$\text{Conversion (\%)} = \frac{\text{mol of reactant charged} - \text{mol of reactant left}}{\text{mol of reactant charged}} \times 100$$

$$\text{Selectivity (\%)} = \frac{\text{mol of product}}{\text{mol of reactant charged} - \text{mol of reactant left}} \times 100$$

3 Results and discussion

3.1 Activity and selectivity in HMF oxidation reaction

Table 1 shows the conversion and selectivity of HMF oxidation on activated carbon (C)-supported Ru, Pt and Pd catalysts in the presence of $Mg(OH)_2$ as a base additive at 383 K and 1.0 MPa O_2. For comparison, ZrO_2, TiO_2 and Al_2O_3-supported Ru catalysts were also examined. While C is frequently used as an inert support for noble metal catalysts in HMF oxidation [26], ZrO_2, TiO_2 and Al_2O_3 are widely used supports in alcohol oxidation reactions [27]. TEM images and size distributions for these catalysts are displayed in Figure 1, showing that their metal particles were well dispersed and possessed similar mean diameters of 1.1–2.1 nm.

For the selective oxidation of HMF, it is known that FDCA is a secondary oxidation product via 2,5-diformylfuran (DFF) intermediate, and its selectivity generally increases with increasing the HMF conversions in the presence of base additives [25]. Therefore, the different catalysts in Table 1 were compared at full conversion of HMF, in order to rigorously

Table 1 HMF conversion and product selectivity of activated carbon-supported Pt, Pd and different supported Ru catalysts in aerobic oxidation of HMF [a)]

Entry	Catalyst [b)]	HMF conversion (%)	Selectivity (%)		Carbon balance (%)
			FDCA	FFCA	
1	Ru/C	100	97.3	0	97.3
2	Pt/C	100	73.4	18.2	91.6
3	Pd/C	100	33.1	52.3	85.4
4	Ru/ZrO_2 [c)]	100	82.2	4.1	86.3
5	Ru/TiO_2 [c)]	100	80.8	5.3	86.1
6	Ru/Al_2O_3 [c)]	100	86.1	1.9	88.0

a) Reaction conditions: 383 K, 8 h, 1.0 MPa O_2, 0.1 g HMF, HMF/metal=40:1 (molar ratio), 20 mL H_2O, 0.2 g $Mg(OH)_2$; b) 5.0 wt% metal loading; c) HMF/metal=30:1 (molar ratio).

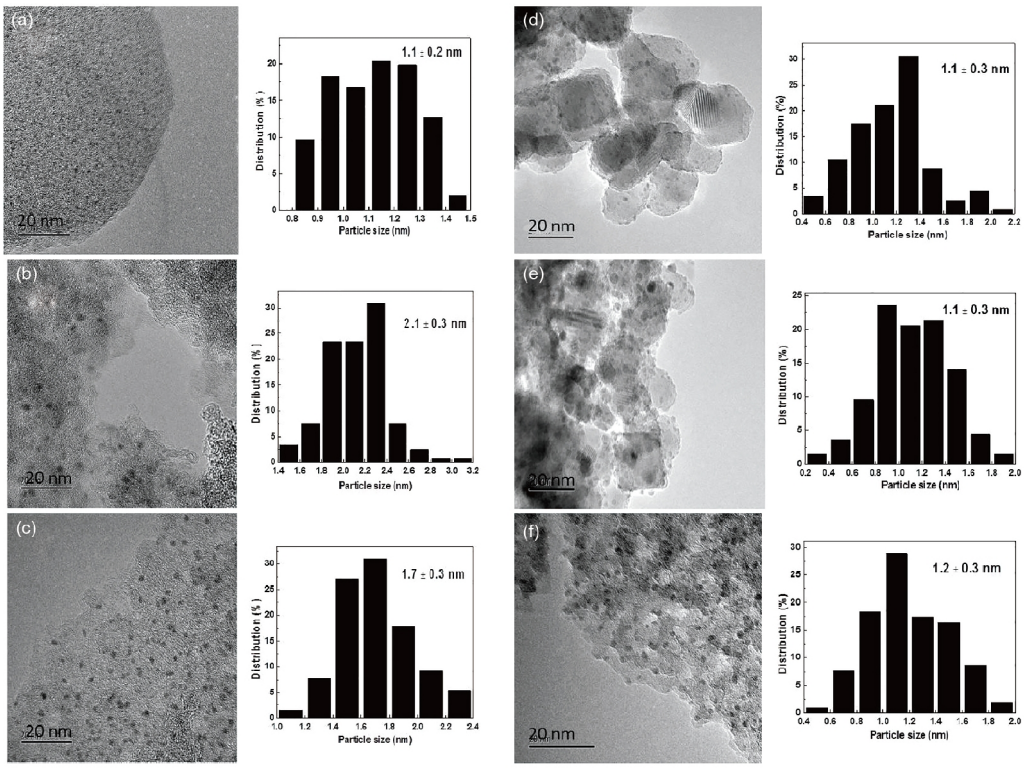

Figure 1 TEM images (scale bar=20 nm) and size distributions of different metal catalysts. (a) Ru/C; (b) Pt/C; (c) Pd/C; (d) Ru/ZrO_2; (e) Ru/TiO_2; (f) Ru/Al_2O_3.

show their efficiency in the formation of FDCA. As shown in Table 1 (entries 1–3), Ru/C was selective to FDCA at 383 K and 1.0 MPa O_2, and as the only product detected by HPLC, its selectivity reached as high as 97.3% (entry 1) at 100% HMF conversion after reaction for 8 h, corresponding to its yield of 97.3%. The FDCA selectivity was much higher than that on Pt/C and Pd/C, being 73.4% and 33.1%, respectively, under the identical reaction conditions. Pt/C and Pd/C also led to the formation of 5-formyl-2-furancarboxylic acid (FFCA) with a selectivity of 18.2% and 52.3%, respectively (entries 2 and 3), revealing that Pt/C and Pd/C are inferior to Ru/C in the selective oxidation of HMF to FDCA.

To examine the support effect, similar Ru nanoparticles (1.1–1.2 nm) with narrow size distributions, as shown in Figure 1, were prepared on the four different supports. Ru/ZrO_2, Ru/TiO_2 and Ru/Al_2O_3 exhibited lower activity, and thus in order to reach the full conversion of HMF, they required lower HMF/metal molar ratio of 30/1, relative to 40/1 used for Ru/C (Table 1, entries 1 and 4–6). Moreover, they were less selective for the formation of FDCA, and the FDCA selectivities fell in the range of 81%–86%. Ru/Al_2O_3 achieved a higher FDCA selectivity (86.1%) than Ru/ZrO_2 (82.2%) and Ru/TiO_2 (81.1%). In addition, it is noted that the ZrO_2, TiO_2, and Al_2O_3 supports led to lower carbon balance (86.1%–88.0% vs. 97.3%), although the underlying reason was not clear, which may be attributed to the favored formation of unidentified degradation and polymerization byproducts on their surfaces, compared with the inert C surface [28]. Such comparison reflects that C is the most preferable support, at least, in the oxidation of HMF.

Using Ru/C (with 5 wt% Ru loading) as the catalyst, different base additives were examined, in addition to $Mg(OH)_2$, in the selective oxidation of HMF to FDCA. As shown in Table 2, in the absence of any bases (entry 1), FDCA and FFCA were formed in selectivities of 52.2% and 38.4%, respectively, and the carbon balance was around 90.6% at 100% HMF conversion. This result is different from that in the presence of $Mg(OH)_2$, as discussed above, and FDCA was the only detected product with a selectivity of 97.3% (entry 2). HT was found to be efficient for the HMF oxidation to FDCA in our previous work [25], and the selectivity of FDCA reached 78.2% in the presence of HT (Mg/Al=3), similar to the result (76.4%, entry 4) in this work. When the Mg/Al ratio of HT increased to 4 (entry 3), the FDCA selectivity increased to 89.6%, and no FFCA was detected. However, when the Mg/Al ratio decreased to 2 (entry 5), the FDCA selectivity decreased to 73.3% with 5.1% FFCA selectivity. Using Al_2O_3 and $Al(OH)_3$ instead, the FDCA selectivities were 47.1% and 62.3% respectively (entries 6 and 7). The presence of La_2O_3 led to the dominant formation of FFCA with a selectivity of 60.5% while the FDCA selectivity was only 25.1% (entry 8). Contrary to La_2O_3, $CaCO_3$ with stronger basicity offered the FDCA and FFCA selectivities were 61.9% and 23.3%, respectively (entry 9). When NaOH and Na_2CO_3 were added (entries 10 and 11), FDCA was solely formed but with low selectivities of around 70%. Meanwhile, the low carbon balances (~70%) and the brown color of the reaction solutions reflect that their strong basicity facilities the formation of humins from HMF through its ring-opening and polymerization reactions [29,30]. Based on these results, it is clear that the base additives act as not only neutralizers to stabilize FDCA, but also promotors for the oxidation of HMF and particularly FFCA intermediate to FDCA.

It is noted that the efficiency of the Ru/C catalyst in the formation of FDCA strongly depends on its Ru loading (Figure 2). To examine such dependence more clearly, the HMF reaction time was shortened to 4 h from 8 h, the time generally employed in this work. C support was inactive for the HMF oxidation, and the conversion and FDCA yield were less than 1% after 4 h. Under the identical conditions, loading 0.5 wt% Ru on C support led to a 100% HMF conversion, and dominant formation of FDCA and FFCA in

Table 2 Effect of base additives on HMF conversion and product selectivity of Ru/C in aerobic oxidation of HMF [a)]

Entry	Base additive	HMF conversion (%)	Selectivity (%)		Carbon balance (%)
			FDCA	FFCA	
1	none	100	52.2	38.4	90.6
2	$Mg(OH)_2$	100	97.3	0	97.3
3	HT (Mg/Al=4)	100	89.6	0	89.6
4	HT (Mg/Al=3)	100	76.4	0	76.4
5	HT (Mg/Al=2)	100	73.3	5.1	78.4
6	Al_2O_3	100	47.1	15.3	62.4
7	$Al(OH)_3$	100	62.3	4.5	66.8
8	La_2O_3	100	25.1	60.5	85.6
9	$CaCO_3$	100	61.9	23.3	85.2
10	NaOH	100	72.3	0	72.3
11	Na_2CO_3	100	68.5	1.2	69.7

a) Reaction conditions: 383 K, 8 h, 1.0 MPa O_2, 0.1 g HMF, HMF/metal=40:1 (molar ratio), 20 mL H_2O, 0.2 g base.

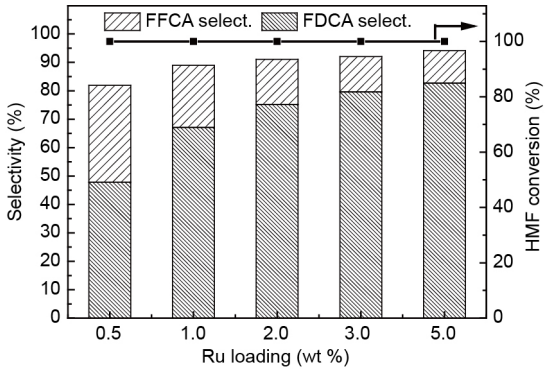

Figure 2 Effect of Ru loading of Ru/C catalysts on their catalytic performances in the aerobic oxidation of HMF to FDCA. Reaction conditions: 383 K, 4 h, 1.0 MPa O_2, 0.1 g HMF, HMF/metal=40:1 (molar ratio), 20 mL H_2O, 0.2 g $Mg(OH)_2$.

47.8% and 34.1% selectivity, respectively. With increasing the Ru loadings from 0.5 wt% to 5.0 wt%, the FDCA selectivity increased from 47.8% to 82.7%, while the FFCA selectivity concurrently decreased from 34.1% to 11.4% (Figure 2). For these Ru/C catalysts with different Ru loadings, the Ru nanoparticles were well dispersed on the C support surface and the mean sizes were similar (1.0–1.1 nm), as shown in Figures 1(a) and 3. Therefore, the difference in the FDCA selectivity for these catalysts is clearly not due to the difference in the size of the Ru nanoparticles, and the consequent effect on their oxidation activity. Further studies indicate that the observed lower FDCA selectivity at lower Ru loadings appears to be related to the presence of excess C support when compared at a given amount of Ru. One such experiment was carried out using a physical mixture of Ru/C (with 5 wt% Ru loading) and C support. By keeping the total C amount equal to that for Ru/C with 0.5 wt% Ru loading, the FDCA selectivity declined to 54.7% with the increase in the FFCA selectivity to 29.1%, close to the values of Ru/C with 0.5 wt% Ru loading. Such negative effect of excess C support appears to be due to its strong adsorption of FFCA intermediate and thus the prohibited oxidation of FFCA on Ru surface to FDCA. Taken together, these results suggest that the higher Ru loadings, while maintaining the higher dispersion of Ru nanoparticles, on C support are beneficial to the oxidation of HMF to FDCA.

The stability and recyclability of the Ru/C catalysts were also examined in the HMF oxidation. Figure 4 shows the representative results on Ru/C with 5 wt% Ru loading at 383 K and 1.0 MPa O_2 in the presence of $Mg(OH)_2$. The HMF conversion remained to be 100%, and FDCA was the only detected product and its selectivity hardly changed over the six cycles. Inductively coupled plasma-atomic emission spectrometry (ICP-AES) analysis showed no detectable leaching of Ru species in the reaction solution after six cycles. Characterization of the catalyst by TEM (Figure 5) shows no essential change in the size distribution and the mean size of the Ru nanoparticles (1.1±0.3 nm) after six cycles, compared with the fresh Ru/C catalyst (1.1±0.2 nm, Figure 1(a)). These results demonstrate that Ru/C is stable and recyclable under the reaction conditions in this work.

3.2 Effects of reaction parameters on selective oxidation of HMF to FDCA

Figure 6 shows the evolution of the HMF conversion and product selectivity with the reaction time at 383 K and 1.0 MPa O_2. It is noted that at the very beginning, the HMF conversion reached 73.2% with the dominant formation of DFF (51.2%) and FFCA (31.3%), and FDCA was not detected. Such observed HMF conversion was contributed from the

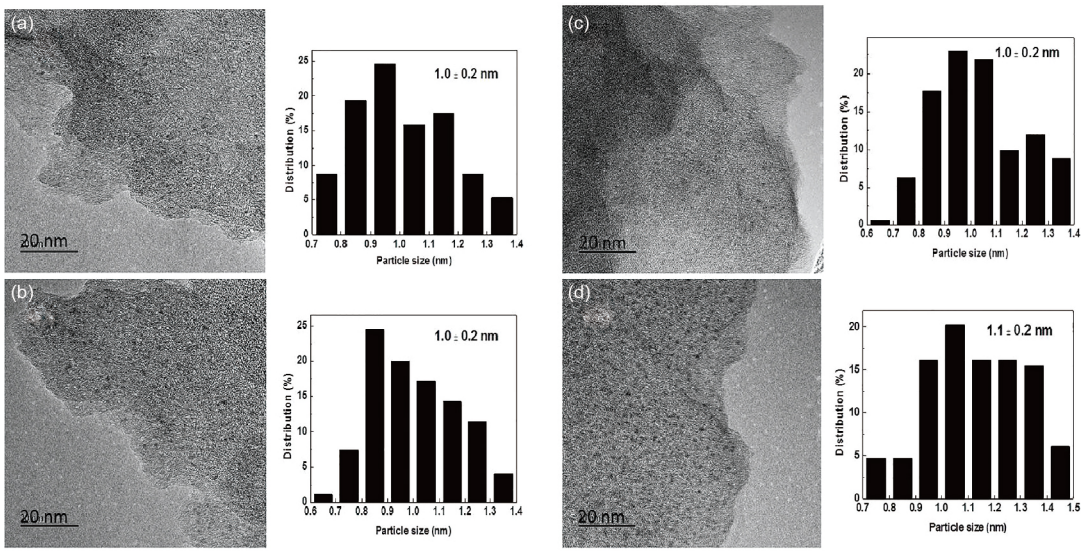

Figure 3 TEM images (scale bar=20 nm) and size distributions of Ru/C catalysts with different Ru loadings. (a) 0.5 wt%; (b) 1.0 wt%; (c) 2.0 wt%; (d) 3.0 wt%.

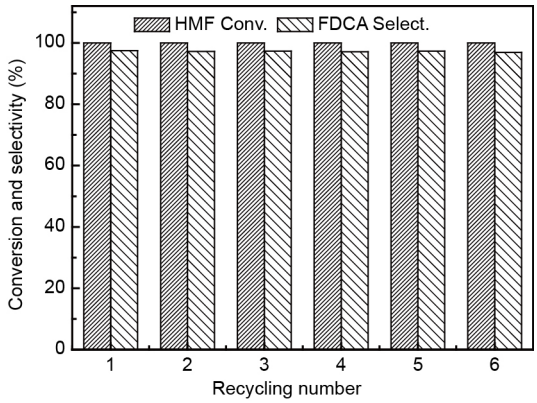

Figure 4 HMF conversion and FDCA selectivity for six reaction cycles on Ru/C (with 5 wt% Ru loading). Reaction conditions: 383 K, 8 h, 1.0 MPa O_2, 0.1 g HMF, HMF/metal=40:1 (molar ratio), 20 mL H_2O, 0.2 g $Mg(OH)_2$.

heating process that lasted about 20 min to reach 383 K from 298 K. After reaction for 0.5 h at 383 K, the HMF conversion increased from 73.2% to 100%, and the DFF selectivity decreased sharply from 51.2% to 0. Differently, the FFCA selectivity first increased from 31.3% to 76.1% during the first 0.5 h, and then decreased to 11.4% after 4 h, and ultimately to 0 when the reaction time was further prolonged to 8 h. The FDCA selectivity increased rapidly from 0 to 82.7% within 4 h, and then gradually approached the maximum value of 97.9% after reaction for 12 h. These results suggest that DFF is formed as the primary product for the HMF oxidation, which is subsequently oxidized to FFCA; FFCA is the key intermediate for FDCA.

Higher reaction temperatures and O_2 pressures can accelerate the oxidation of FFCA to FDCA on Ru/C. As shown in Figure 7, the HMF conversion remained to be 100% at 343–423 K. However, when the temperature increased from 343 K to 403 K, the FDCA selectivity increased from 2.9% to 92.6% concurrently with the decrease in the FFCA selectivity from 90.5% to 0. Further increase in the temperature to 423 K led to a slight decrease in the FDCA selectivity to 89.3%, most likely due to the poor stability of HMF and its favored condensation and degradation reactions to some unidentified byproducts at higher temperatures.

Figure 8 shows that the HMF conversion remained to be 100% in the O_2 pressure range 0.2–1.5 MPa. With increasing the O_2 pressure from 0.2 MPa to 1.0 MPa, the FDCA selectivity increased from 52.0% to 82.7%, and the FFCA selectivity decreased from 41.5% to 11.4%, which then remained the same up to 1.5 MPa.

3.3 Reaction pathways for aerobic oxidation of HMF to FDCA

For the aerobic oxidation of HMF to FDCA on different supported metal catalysts, it can proceed following two alternative routes, differing in the primary oxidation of the hydroxyl group of HMF to DFF or its aldehyde group to 5-hydroxymethyl-2-furancarboxylic acid (HMFCA) intermediate [31–36]. As shown in Figure 6, HMFCA was not detected, and DFF formed as the primary product on Ru/C in the presence of $Mg(OH)_2$. Taken together with the observed effect of reaction temperature and O_2 pressure (Figures 7 and 8), we tentatively propose the reaction pathways for the aerobic oxidation of HMF to FDCA, as depicted in Scheme 1, involving DFF intermediate, rather than HMFCA, which then undergoes sequential oxidation to FFCA and FDCA. Comparing the evolution trends of DFF, FFCA and FDCA with time (Figure 6), obviously, the formation of DFF and its oxidation to FFCA occurred much faster than the oxidation of FFCA to FDCA, which indicates that the conversion of FFCA to FDCA is the rate-limiting step in the oxidation of HMF.

To verify such proposition, the individual reaction steps involved in the oxidation of HMF to FDCA were studied on

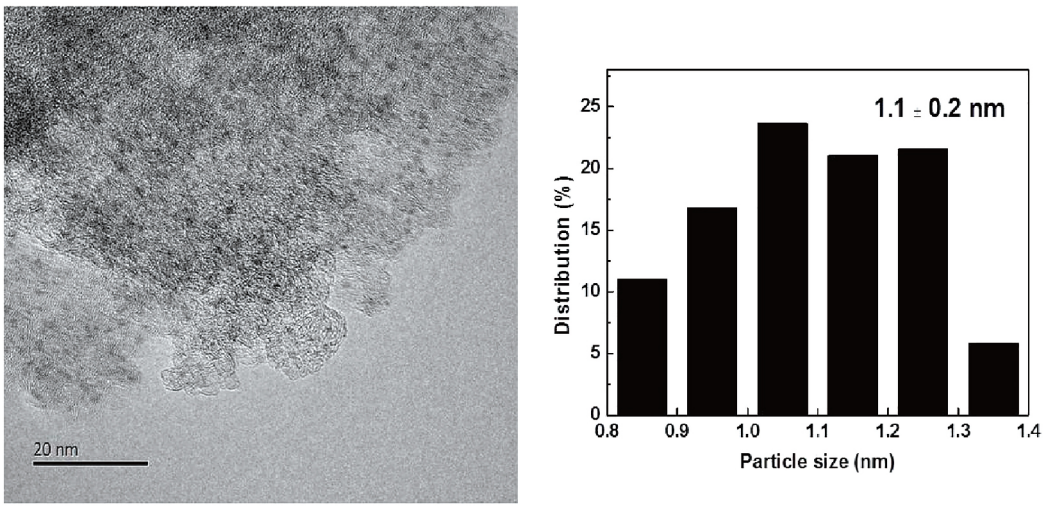

Figure 5 TEM image (scale bar=20 nm) and size distribution of Ru/C after six reaction cycles.

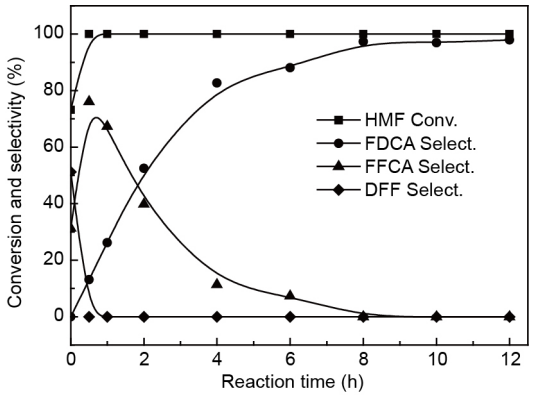

Figure 6 Effect of the reaction time on the catalytic performances of Ru/C in aerobic oxidation of HMF. Reaction conditions: 383 K, 1.0 MPa O_2, 0.1 g HMF, HMF/metal=40:1 (molar ratio), 20 mL H_2O, 0.2 g $Mg(OH)_2$.

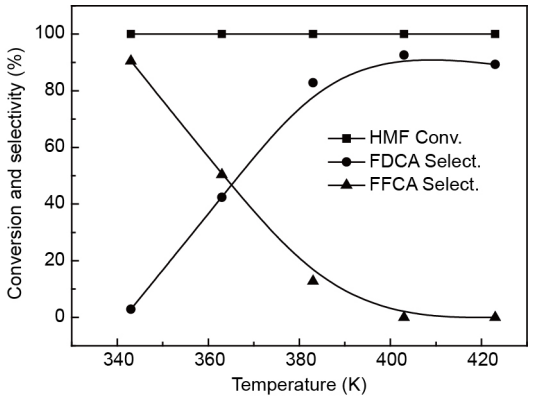

Figure 7 Effect of reaction temperature on product selectivity on Ru/C at 100% HMF conversion. Reaction conditions: 383 K, 4 h, 1.0 MPa O_2, 0.1 g HMF, HMF/metal=40:1 (molar ratio), 20 mL H_2O, 0.2 g $Mg(OH)_2$.

Ru/C (with 5 wt% Ru loading). As shown in Table 3, the rate constant of FFCA oxidation to FDCA (2.49×10^{-6} s^{-1}) was much smaller than those of HMF oxidation to DFF (9.15×10^{-5} s^{-1}) and DFF to FFCA (8.05×10^{-5} s^{-1}). Accordingly, the oxidation of FFCA to FDCA possessed the higher activation energy (52.5 kJ/mol), compared with the other two oxidation steps of HMF to DFF (34.2 kJ/mol) and DFF to FFCA (38.6 kJ/mol). Therefore, the oxidation of FFCA to FDCA as the rate-determining step dictates the formation rate of FDCA from HMF on Ru/C.

Figure 8 Effect of O_2 pressure on the catalytic performances of Ru/C. Reaction conditions: 383 K, 4 h, 0.1 g HMF, HMF/metal=40:1 (molar ratio), 20 mL H_2O, 0.2 g $Mg(OH)_2$.

4 Conclusions

Activated carbon supported Ru nanoparticles (~1 nm) are efficient and stable in the aerobic oxidation of HMF to FDCA in the presence of $Mg(OH)_2$ as a base additive, offering a high FDCA yield of 97% at 383 K and 1.0 MPa O_2. Ru/C is superior to Pt/C and Pd/C and also the other supported Ru catalysts (including Ru/ZrO_2, Ru/TiO_2 and Ru/Al_2O_3) for the formation of FDCA under the same reaction conditions. Higher Ru loadings on C support facilitate the HMF oxidation to FDCA

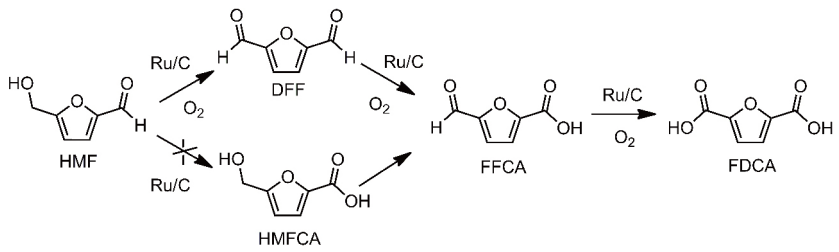

Scheme 1 Reaction pathways for aerobic oxidation of HMF to FDCA on Ru/C.

Table 3 Rate constant and apparent activation energy for aerobic oxidation of HMF, DFF and FFCA on Ru/C catalyst [a)]

Reaction	k (s^{-1}) [b)]	E_a (kJ/mol) [c)]
Oxidation of HMF to DFF	9.15×10^{-5}	34.2
Oxidation of DFF to FFCA	8.05×10^{-5}	38.6
Oxidation of HMF to FDCA	2.49×10^{-6}	52.5

a) Reaction conditions: 1.0 MPa O_2, 0.1 g substrate, substrate/metal=40:1 (molar ratio), 20 mL H_2O, 0.2 g $Mg(OH)_2$; b) reaction at 313 K (reaction rate constants were estimated by assuming a first-order reaction in HMF and DFF); c) reaction at 303–333 K (activation energy was calculated by the Arrhenius equation).

in the range of 0.5 wt%–5.0 wt%. Base additives act as not only neutralizers for FDCA, but also promotors for the oxidation of HMF to FDCA. It is confirmed that the oxidation of HMF to FDCA is preceded by oxidation of its hydroxyl group to DFF intermediate, and the oxidation of FFCA to FDCA is the rate-determining step.

Acknowledgments This work was supported by the National Natural Science Foundation of China (21373019, 21433001, 21690081).

Conflict of interest The authors declare that they have no conflict of interest.

1 Chheda JN, Huber GW, Dumesic JA. *Angew Chem Int Ed*, 2007, 46: 7164–7183
2 Corma A, Iborra S, Velty A. *Chem Rev*, 2007, 107: 2411–2502
3 Zhang X, Murria P, Jiang Y, Xiao W, Kenttämaa HI, Abu-Omar MM, Mosier NS. *Green Chem*, 2016, 18: 5219–5229
4 Qi X, Watanabe M, Aida TM, Smith Jr RL. *Green Chem*, 2008, 10: 799–805
5 Yang F, Liu Q, Yue M, Bai X, Du Y. *Chem Commun*, 2011, 47: 4469–4471
6 Román-Leshkov Y, Chheda JN, Dumesic JA. *Science*, 2006, 312: 1933–1937
7 Amarasekara AS, Green D, Williams LTD. *Eur Polymer J*, 2009, 45: 595–598
8 Gandini A, Silvestre AJD, Neto CP, Sousa AF, Gomes M. *J Polym Sci A Polym Chem*, 2009, 47: 295–298
9 Moreau C, Belgacem MN, Gandini A. *Chem Inform*, 2004, 35: 11–30
10 Partenheimer W, Grushin VV. *Adv Synth Catal*, 2001, 343: 102–111
11 Sahu R, Dhepe PL. *Reac Kinet Mech Cat*, 2014, 112: 173–187
12 Miao Z, Wu T, Li J, Yi T, Zhang Y, Yang X. *RSC Adv*, 2015, 5: 19823–19829
13 Verdeguer P, Merat N, Gaset A. *J Mol Catal*, 1993, 85: 327–344
14 Casanova O, Iborra S, Corma A. *ChemSusChem*, 2009, 2: 1138–1144
15 Siyo B, Schneider M, Radnik J, Pohl MM, Langer P, Steinfeldt N. *Appl Catal A-Gen*, 2014, 478: 107–116
16 Mei N, Liu B, Zheng J, Lv K, Tang D, Zhang Z. *Catal Sci Technol*, 2015, 5: 3194–3202
17 Ait Rass H, Essayem N, Besson M. *Green Chem*, 2013, 15: 2240–2251
18 Pasini T, Piccinini M, Blosi M, Bonelli R, Albonetti S, Dimitratos N, Lopez-Sanchez JA, Sankar M, He Q, Kiely CJ, Hutchings GJ, Cavani F. *Green Chem*, 2011, 13: 2091
19 Gupta NK, Nishimura S, Takagaki A, Ebitani K. *Green Chem*, 2011, 13: 824–827
20 Gorbanev YY, Kegnæs S, Riisager A. *Catal Lett*, 2011, 141: 1752–1760
21 Artz J, Palkovits R. *ChemSusChem*, 2015, 8: 3832–3838
22 Yi G, Teong SP, Zhang Y. *Green Chem*, 2016, 18: 979–983
23 Nie J, Xie J, Liu H. *J Catal*, 2013, 301: 83–91
24 Nie J, Xie J, Liu H. *Chin J Catal*, 2013, 34: 871–875
25 Xie J, Nie J, Liu H. *Chin J Catal*, 2014, 35: 937–944
26 Davis SE, Zope BN, Davis RJ. *Green Chem*, 2012, 14: 143–147
27 Nie J, Liu H. *Pure Appl Chem*, 2011, 84: 765–777
28 Pupovac K, Palkovits R. *ChemSusChem*, 2013, 6: 2103–2110
29 Kerdi F, Ait Rass H, Pinel C, Besson M, Peru G, Leger B, Rio S, Monflier E, Ponchel A. *Appl Catal A-Gen*, 2015, 506: 206–219
30 Davis SE, Houk LR, Tamargo EC, Datye AK, Davis RJ. *Catal Today*, 2011, 160: 55–60
31 Zope BN, Davis SE, Davis RJ. *Top Catal*, 2012, 55: 24–32
32 Albonetti S, Lolli A, Morandi V, Migliori A, Lucarelli C, Cavani F. *Appl Catal B-Environ*, 2015, 163: 520–530
33 Vuyyuru KR, Strasser P. *Catal Today*, 2012, 195: 144–154
34 Chadderdon DJ, Xin L, Qi J, Qiu Y, Krishna P, More KL, Li W. *Green Chem*, 2014, 16: 3778–3786
35 Wan X, Zhou C, Chen J, Deng W, Zhang Q, Yang Y, Wang Y. *ACS Catal*, 2014, 4: 2175–2185
36 Zhou C, Deng W, Wan X, Zhang Q, Yang Y, Wang Y. *ChemCatChem*, 2015, 7: 2853–2863